Research on Motion Control of Underwater Robots Based on Sliding Mode Control

Xuqing Liu *, Jie Yu, Xinzhu Li, Changqin Chen, Xiao Chen, Xin Deng

Oil Production Service Branch of CNOOC Energy Technology & Services Limited, Tianjin, China

* Corresponding Author Email: liuxq28@cnooc.com.cn

Abstract. The ocean harbors abundant mineral resources, and underwater robots, serving as critical tools for the exploration and exploitation of subsea resources, exhibit significant developmental potential. However, the complexity of marine environments poses substantial challenges for achieving precise control of these systems. This study implements a sliding mode variable structure control (SMVSC) algorithm into the autonomous control framework of remotely operated vehicles (ROVs), integrating a saturation function to suppress chattering phenomena. Simulation results demonstrate that the proposed sliding mode controller outperforms conventional PID and fuzzy PID controllers in terms of stability and robustness. Experimental validation through depth and heading stabilization tasks confirmed the efficacy and reliability of the control strategy. The findings of this research advance the field of underwater robotics by offering a robust theoretical framework and practical methodology for enhancing stable control in dynamic marine environments.

Keywords: Sliding Mode Control (SMC); Underwater Robots; Stability Control; Motion Control.

1. Introduction

Underwater robots, also known as underwater vehicles, are intelligent tools that can replace divers to complete various underwater tasks. Currently, underwater robots play important roles in fields such as marine fishing, marine resource exploration and development, underwater search and rescue, and marine biological sampling [1-4]. Achieving precise motion control is essential for underwater robots to successfully execute their assigned tasks. This capability necessitates the robotic system to rapidly converge to the desired position while maintaining stable positioning upon arrival. Consequently, motion control methodologies have become a focal point in underwater robotics research, with control system design representing a critical component in the development of such robotic systems. Investigators have explored diverse control strategies, yielding varying levels of control performance, which can be broadly categorized as follows:

(1) PID control is a classic linear system control method widely used in industrial control. Qi Shengbo et al. applied fuzzy PID to the depth - keeping motion control of a small - sized ROV. Through Simulink simulation, its overshoot was 7.8% and the adjustment time was 26.71 s. Junjie Dong et al. [5] proposed a type - 2 fuzzy PID control. After simulation analysis, its overshoot was 0.3% and the adjustment time was 7.5 s. Through comparative simulation, it was verified that its control effect was better than that of ordinary fuzzy PID control [6].

(2) Model predictive control is an advanced control technology widely applied in fields such as automotive control, aerospace control, and robot control. Wang Mingyang [7] proposed an MPC - based ROV inspection trajectory tracking control method. A simulation platform was built using ROS for simulation experiments. The simulation results showed that under the given constraint conditions, the ROV operated smoothly, had a good trajectory tracking control effect, and could successfully complete the observation task. Chengqi Long et al. [8] constructed a state - based extended Kalman filter (ESKF) for the trajectory tracking problem of underwater robots and proposed a model predictive control (MPC) controller based on ESKF. Finally, the effectiveness of the proposed method was verified through simulation analysis. M.P.R.Prasad et al. [9] attempted to apply model predictive control to the position tracking and speed control of an ROV. The research object was the remotely operated underwater vehicle 'Kaxan' developed by CIDESI in Mexico. The linear quadratic regulator (LQR) method was used to process the ROV system model, and model predictive control was further

applied to improve the position and speed control of the ROV. The simulation results showed that the MPC algorithm had a good control effect and stability.

(3) Sliding mode control (SMC) is a non - linear control method. Yang Jianhua et al. [10] applied sliding mode control (SMC) to the depth - keeping control of underwater robots. A model was established in Simulink for simulation. The effects of the SMC algorithm and the PID algorithm were compared at different navigation speeds. The results showed that SMC had a better control effect. Govinda et al. [11] combined second - order sliding mode control (2nd - SMC) with back - propagation neural network (BP - NN) to propose a neuro - sliding control method (NSC) and applied it to a small - sized ROV for experiments, achieving good control results. ZongSheng Wang et al. [12] combined the adaptive control method with the sliding mode control method to propose an adaptive sliding mode motion controller (ASM controller). The sliding mode controller was designed using the exponential reaching law, and a saturation function was added to eliminate chattering. Malte von Benzon et al. [13] applied the sliding mode control (SMC) algorithm to an ROV with a water - jet cleaning function, enabling the ROV to track the target depth trajectory and maintain stability when the water - jet was activated.

(4) Active Disturbance Rejection Control (ADRC) is a new - type control method improved based on PID control, often used in problems such as robot control and UAV attitude control. Shen Yuxuan et al. [14] applied the ADRC controller to the motion control of underwater robots. The effectiveness of the control algorithm was verified through simulation analysis, and it was compared with the PID controller. The results showed that the ADRC controller had a better effect than the PID controller. Chen Zengqiang et al. [15] applied the linear active disturbance rejection control (LADRC) method to the motion control of underwater robots. Compared with the PID control method, the LADRC method reduced the relative error of the robot's depth control from 3.5% to 0.5%, improving the control accuracy and stability.

This paper aims to explore the research status and development trends of underwater robot control algorithms. The sliding - mode variable - structure control algorithm is applied to the automatic control function of ROVs, and a saturation function is introduced to weaken the adverse effects caused by the chattering phenomenon. Compared with traditional control algorithms, accuracy and stability are improved. Through simulation and experimental verification, it is verified that the proposed algorithm exhibits superior robustness and stability in complex underwater environments, providing theoretical support and technical reference for the practical application of underwater robots.

2. Dynamic Model

Establishing a mathematical model for the Remotely Operated Vehicle (ROV) is a crucial foundation for its research and application. The mathematical model helps describe the robot's state, analyzes its physical characteristics and kinematic laws, and is also a prerequisite for subsequent motion control. In the dynamic analysis of the ROV, the rigid body dynamic model is first established, ignoring hydrodynamic forces, and treating the ROV as a rigid body. Based on the momentum theorem and the momentum theorem for rigid bodies, the following equations are obtained:

$$\frac{dB}{dt} = F \qquad \frac{dL}{dt} = M \tag{1}$$

$$m[\frac{dv_1}{dt} + v_2 \times v_1 + \frac{dv_2}{dt} \times r_G + v_2 \times (v_2 \times r_G)] = F \tag{2}$$

$$I_0[\frac{dv_2}{dt} + v_2 \times (I_0 v_2) + m r_G \times (\frac{dv_1}{dt} + v_2 \times v_1)] = M \tag{3}$$

Where r_G is the coordinate of the center of gravity of the ROV, $r_G = (x_G, y_G, z_G)$; v_1 and v_2 are the linear and angular velocities of the ROV under moving sy, $v_1 = (u, v, w)$ $v_2 = (p, q, r)$; τ are the forces and torques experienced by the ROV body, $F=(X,Y,Z)$ $M=(K,M,N)$; I_0 is ROV rotational inertia matrix, $I_0=\begin{bmatrix} I_x & -I_{xy} & -I_{xz} \\ -I_{xy} & I_y & -I_{yz} \\ -I_{xz} & -I_{yz} & I_z \end{bmatrix}$; I_x, I_y, I_z are the moment of inertia I_{xy}, I_{xz}, I_{yz} are the product of inertia.

Expanding each coefficient in the above equation and substituting them into the original equation yields the complete set of rigid body dynamics equations as follows:

Represent the above system of equations in matrix form:

$$M_{RB}\dot{v}+C_{RB}v=\tau \tag{4}$$

Where MRB is the inertia matrix of the ROV, and CRB is the Coriolis and centripetal matrix caused by the inertia matrix. Their expressions are as follows:

$$M_{RB}=\begin{bmatrix} m & 0 & 0 & 0 & mz_G & -my_G \\ 0 & m & 0 & -mz_G & 0 & mx_G \\ 0 & 0 & m & my_G & -mx_G & 0 \\ 0 & -mz_G & my_G & I_x & I_{xy} & I_{xz} \\ mz_G & 0 & -mx_G & I_{yx} & I_y & I_{yz} \\ -my_G & mx_G & 0 & I_{zx} & I_{zy} & I_z \end{bmatrix} \tag{5}$$

$$C_{RB}=\begin{bmatrix} 0 & 0 & 0 & m(y_Gq+z_Gr) & -m(x_Gq-w) & -m(x_Gr+v) \\ 0 & 0 & 0 & -m(y_Gp+w) & m(z_Gr+x_Gp) & -m(y_Gr-u) \\ 0 & 0 & 0 & -m(z_Gp-v) & -m(z_Gq-u) & m(x_Gp+y_Gq) \\ -m(y_Gq+z_Gr) & m(y_Gp+w) & m(z_Gp-v) & 0 & -I_{yz}q-I_{xz}p+I_zr & I_{yz}r+I_{yy}p-I_zq \\ m(x_Gq-w) & -m(z_Gr+x_Gp) & m(z_Gq+u) & I_{yz}q+I_{zz}p-I_zr & 0 & -I_{zz}r-I_{zy}q+I_{zz}p \\ m(x_Gr+v) & m(y_Gr-u) & -m(x_Gq+y_Gq) & -I_{yz}r-I_{zy}p+I_yq & I_{zz}r+I_{zy}q-I_zp & 0 \end{bmatrix} \tag{6}$$

The simplified inertia matrix and its corresponding Coriolis and centripetal matrix are of the following form:

$$M_{RB}=\begin{bmatrix} m & 0 & 0 & 0 & 0 & 0 \\ 0 & m & 0 & 0 & 0 & 0 \\ 0 & 0 & m & 0 & 0 & 0 \\ 0 & 0 & 0 & I_x & 0 & 0 \\ 0 & 0 & 0 & 0 & I_y & 0 \\ 0 & 0 & 0 & 0 & 0 & I_z \end{bmatrix} \quad C_{RB}=\begin{bmatrix} 0 & 0 & 0 & 0 & mw & -mv \\ 0 & 0 & 0 & -mw & 0 & mu \\ 0 & 0 & 0 & mv & -mu & 0 \\ 0 & mw & -mv & 0 & I_zr & -I_yq \\ -mw & 0 & mu & -I_zr & 0 & I_xp \\ mv & -mu & 0 & I_yq & -I_xp & 0 \end{bmatrix} \tag{7}$$

Then, perform hydrodynamic modeling on the ROV. When the ROV moves in water, the water will exert a reactive force on the ROV. This force is called hydrodynamic force. The hydrodynamic force experienced by the ROV is related to its structure, shape, velocity and acceleration. Generally, the hydrodynamic force acting on the ROV is divided into inertial hydrodynamic force and viscous hydrodynamic force, as shown in the following formula. Here, τA represents the inertial hydrodynamic force. τA is the inertial hydrodynamic force, and τD is the viscous hydrodynamic force.

$$\tau_H=\tau_H(u,v,w,p,q,r,\dot{u},\dot{v},\dot{w},\dot{p},\dot{q},\dot{r}) \tag{8}$$

$$\tau_H=\tau_A+\tau_D \tag{9}$$

The inertial hydrodynamic force is the hydrodynamic force generated by the inertia caused by the change in the body velocity of the ROV when it moves in water. Its magnitude is related to the rate of change of the ROV's moving velocity, that is, its acceleration. The proportionality coefficient is called added mass. Its formula is shown as (11). The added mass represents the mass of the water flow surrounding the ROV's body and accelerating with it during the ROV's movement. The added mass is expressed as the added mass matrix MA and the Coriolis centripetal force matrix CA caused by the added mass matrix. Their forms are shown in equation (12).

$$\tau_A = M_A \dot{v} + C_A v \tag{10}$$

$$M_A = \begin{bmatrix} X_{\dot u} & X_{\dot v} & X_{\dot w} & X_{\dot p} & X_{\dot q} & X_{\dot r} \\ Y_{\dot u} & Y_{i} & Y_{\dot w} & Y_{\dot p} & Y_{\dot q} & Y_{\dot r} \\ Z_{\dot u} & Z_{i} & Z_{\dot w} & Z_{\dot p} & Z_{\dot q} & Z_{\dot r} \\ K_{\dot u} & K_{\dot v} & K_{\dot w} & K_{\dot p} & K_{\dot q} & K_{\dot r} \\ M_{\dot u} & M_{\dot v} & M_{\dot w} & M_{\dot p} & M_{\dot q} & M_{\dot r} \\ N_{\dot u} & N_{\dot v} & N_{\dot w} & N_{\dot p} & N_{\dot q} & N_{\dot r} \end{bmatrix} \tag{11}$$

$$C_A = \begin{bmatrix} 0 & 0 & 0 & 0 & -a_3 & a_2 \\ 0 & 0 & 0 & a_3 & 0 & -a_1 \\ 0 & 0 & 0 & -a_2 & a_1 & 0 \\ 0 & -a_3 & a_2 & 0 & -b_3 & b_2 \\ a_3 & 0 & -a_1 & b_3 & 0 & -b_1 \\ -a_2 & a_1 & 0 & -b_2 & b_1 & 0 \end{bmatrix} \quad \begin{cases} a_1 = X_u u + X_v v + X_w w + X_p p + X_q q + X_r r \\ a_2 = X_v u + Y_v v + Y_w w + Y_p p + Y_q q + Y_r r \\ a_3 = X_v u + X_w v + Z_w w + Z_p p + Z_q q + Z_r r \\ b_1 = X_p u + Y_p v + Z_p w + K_p p + K_q q + K_r r \\ b_2 = X_q u + Y_q v + Z_q w + K_q p + M_q q + M_r r \\ b_3 = X_r u + Y_r v + Z_r w + K_r p + M_r q + N_r r \end{cases} \tag{12}$$

The forms of the simplified added - mass matrix and its Coriolis centripetal force matrix are as follows:

$$\mathbf{M}_A = -\begin{bmatrix} X_{ii} & 0 & 0 & 0 & 0 & 0 \\ 0 & Y_i & 0 & 0 & 0 & 0 \\ 0 & 0 & Z_{ii} & 0 & 0 & 0 \\ 0 & 0 & 0 & K_p & 0 & 0 \\ 0 & 0 & 0 & 0 & M_q & 0 \\ 0 & 0 & 0 & 0 & 0 & N_i \end{bmatrix} \quad \mathbf{C}_A = \begin{bmatrix} 0 & 0 & 0 & 0 & -Z_w w & -Y_v w \\ 0 & 0 & 0 & Z_w w & 0 & -X_i u \\ 0 & 0 & 0 & -Y_v v & X_i u & 0 \\ 0 & -Z_w w & Y_v v & 0 & -N_r r & M_q q \\ Z_w w & 0 & -X_u u & N_r r & 0 & -K_p p \\ -Y_v v & X_u u & 0 & -M_q q & K_p p & 0 \end{bmatrix} \tag{13}$$

Viscous hydrodynamic force is the hydrodynamic force generated by the viscous adhesion between water molecules and the surface of the ROV when the ROV moves in water. The viscous hydrodynamic force is usually related to factors such as the ROV's structural shape, surface material, and movement speed.

The relationship between the magnitude of the viscous hydrodynamic force and the ROV's speed is called the viscous hydrodynamic force coefficient, also known as the fluid damping coefficient. It can be expressed as the sum of the linear damping coefficient matrix and the nonlinear damping coefficient matrix, as shown in formula (15). The forms of the simplified linear coefficient matrix and nonlinear coefficient matrix are shown in equations (16) and (17).

$$\tau_D = D \cdot v \quad D = D_L + D_{NL} \tag{14}$$

$$D_L = -\begin{bmatrix} X_u & 0 & 0 & 0 & 0 & 0 \\ 0 & Y_v & 0 & 0 & 0 & 0 \\ 0 & 0 & Z_w & 0 & 0 & 0 \\ 0 & 0 & 0 & K_p & 0 & 0 \\ 0 & 0 & 0 & 0 & M_q & 0 \\ 0 & 0 & 0 & 0 & 0 & N_r \end{bmatrix} \tag{15}$$

$$D_{NL} = -\begin{bmatrix} X_{u|u|}|u| & 0 & 0 & 0 & 0 & 0 \\ 0 & Y_{v|v|}|v| & 0 & 0 & 0 & 0 \\ 0 & 0 & Z_{w|w|}|w| & 0 & 0 & 0 \\ 0 & 0 & 0 & K_{p|p|}|p| & 0 & 0 \\ 0 & 0 & 0 & 0 & M_{q|q|}|q| & 0 \\ 0 & 0 & 0 & 0 & 0 & N_{r|r|}|r| \end{bmatrix} \tag{16}$$

3. Simulation

3.1. Diving and surfacing motion

The initial phase of the simulation focuses on the ROV's vertical motion dynamics, specifically examining its performance along the z-axis. This simulation is structured into two distinct components. The first segment evaluates the system's ability to achieve and maintain a predetermined depth level, replicating the ROV's depth-holding capability during operational scenarios. Initial conditions are configured with both depth and velocity parameters set to zero, while the simulation duration is established at 50 seconds with a temporal resolution of 0.01 seconds. The target depth for this evaluation is specified as 2 meters. Comparative analysis is performed using three distinct control methodologies: conventional PID control, adaptive fuzzy PID, and sliding mode control. The respective performance characteristics of these control strategies are illustrated in the subsequent graphical representation.

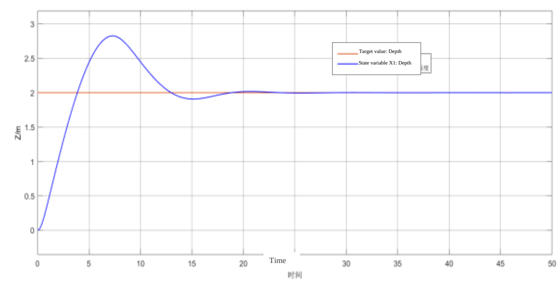

Fig. 1 Simulation diagram of the fixed target value for the diving and surfacing motion using the classical PID algorithm.

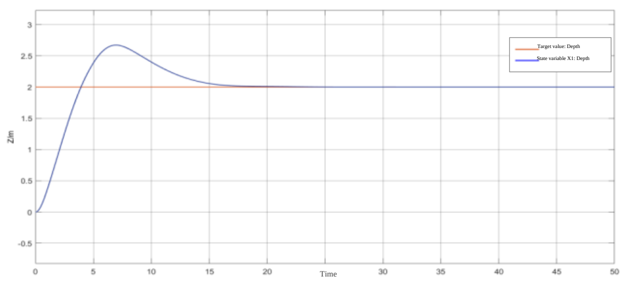

Fig. 2 Simulation diagram of the fixed target value for the diving and surfacing motion using the fuzzy PID algorithm.

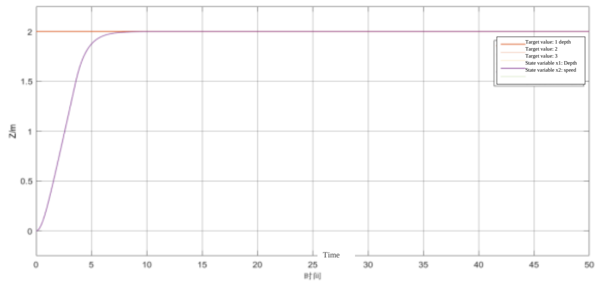

Fig. 3 Simulation diagram of the fixed target value for the diving and surfacing motion under sliding mode control.

After a meticulous examination of the aforementioned images, a comprehensive analysis of the control effects exerted by each controller is conducted. When it comes to the parameter of settling time, the classical PID controller stands out with the longest value, measuring around 23.8 seconds. In contrast, the fuzzy PID controller demonstrates a relatively shorter settling time, which is approximately 18.5 seconds, thus being somewhat more efficient than its classical counterpart. Notably, the sliding mode controller exhibits the most rapid response in terms of settling time, with a value of merely about 8.1 seconds. In practical operational scenarios, the thrust generated by the thruster is subject to an upper - bound limit. In light of this real - world constraint, during the simulation, the output range of the controller is defined within the interval of ±300. This deliberate limitation inevitably leads to a certain degree of elongation in the system's settling time.

Regarding the overshoot phenomenon, the classical PID controller shows a maximum deviation of 0.8, corresponding to an overshoot percentage of 40%. The fuzzy PID controller, on the other hand, has a maximum deviation of 0.67, resulting in an overshoot of 33.5%. Thanks to its unique control characteristics, the sliding mode controller manages to maintain a relatively stable performance without significant overshoot issues.

In summary, within the context of the linear motion-based depth keeping simulation, all three controllers are ultimately capable of achieving system stability. However, there are pronounced differences in their control performances. Among them, the sliding mode controller emerges as the most effective one, followed by the fuzzy PID controller, while the classical PID controller displays the least satisfactory performance.

3.2. Yawing motion

The rotational dynamics of the ROV about its vertical axis were investigated through computational modeling. This simulation study, analogous to previous investigations, was structured to evaluate two distinct operational scenarios: static reference orientation and dynamic angular positioning.

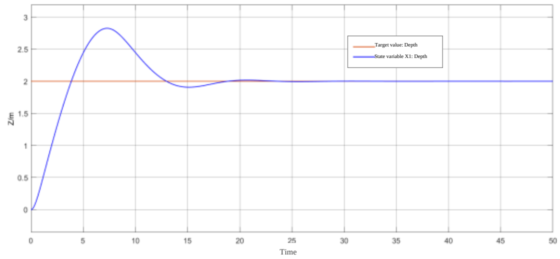

Fig. 4 Simulation diagram of the fixed target value for the yawing motion using the classical PID

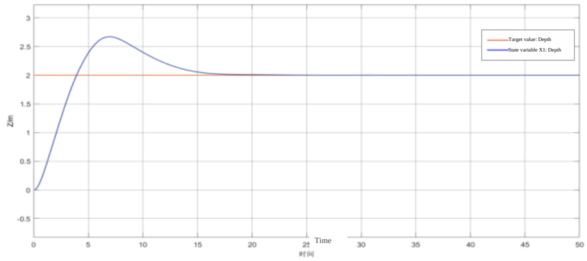

Fig. 5 Simulation diagram of the fixed target value for the yawing motion using the fuzzy PID algorithm.

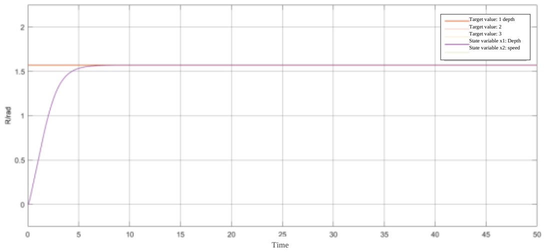

Fig. 6 Simulation diagram of the fixed target value for the diving and surfacing motion under sliding mode control.

The initial simulation phase focused on assessing the system's azimuth stabilization capability under constant reference conditions. The angular displacement was quantified in radians, with the target orientation established at π/2 radians (equivalent to 90°). The simulation parameters were initialized with the ROV at zero angular displacement and stationary condition (ω = 0 rad/s). The temporal domain was configured with a 50-second observation window and a temporal resolution of 0.01 seconds. Comparative performance analysis was conducted using three distinct control methodologies, with the resultant system behaviors graphically represented in subsequent figures.

Through comprehensive analysis of the simulation results and performance metrics, the yaw control evaluation was conducted with the controller's output range constrained to ±300 units. The temporal response characteristics reveal distinct performance differences among the controllers. The conventional PID controller demonstrates the most prolonged stabilization duration, requiring approximately 15.5 seconds to reach steady-state conditions. The adaptive fuzzy PID implementation exhibits marginally extended stabilization characteristics compared to its conventional counterpart, with a settling time of 17.5 seconds. In contrast, the sliding mode controller achieves superior temporal performance, stabilizing within 7.5 seconds, representing a significant reduction in settling time relative to both PID-based implementations. Regarding transient response characteristics, the conventional PID controller manifests a peak deviation of 0.48 radians, corresponding to an overshoot magnitude of 30.6%. The fuzzy PID implementation shows improved performance with a maximum deviation of 0.41 radians and an overshoot of 26.1%. Notably, the sliding mode controller demonstrates exceptional transient behavior, effectively eliminating observable overshoot phenomena. The comparative analysis of yaw stabilization performance under fixed reference conditions indicates that the fuzzy PID controller's characteristics are comparable to those of the conventional PID implementation. However, the sliding mode control strategy exhibits superior performance metrics, particularly in both transient response and stabilization time domains, outperforming both PID-based controllers significantly.

4. Experiment and verification

(a) ROV depth-keeping experiment

The experimental results were systematically processed and evaluated, with the corresponding data visualization presented in Figure 8. During the depth maintenance phase, the ROV system demonstrated a stabilization period of 9 seconds before achieving steady-state operation. Post-stabilization analysis revealed precise position maintenance capabilities, with positional deviations consistently constrained within a ±0.025-meter tolerance range. These empirical findings substantiate the effectiveness of the implemented depth control mechanism, confirming its compliance with both design specifications and operational performance criteria.

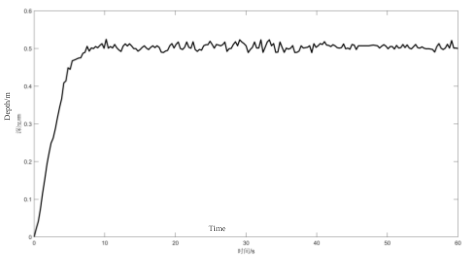

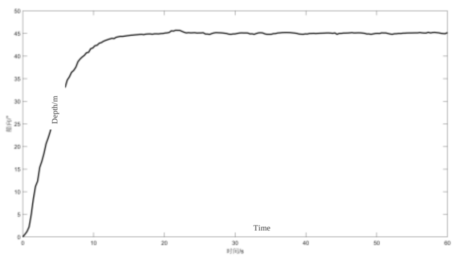

Fig. 7 Data of the depth-keeping experiment **Fig. 8** Data from the Heading Keeping Experiment

(b) ROV yaw-keeping experiment

The ROV yaw-keeping experiment is carried out. Instructions are sent through the upper computer software to execute the yaw-keeping function. The ROV is adjusted so that its initial yaw angle is 0°, and the target yaw angle is set to 45°. Observe the change of the heading angle from the monitoring interface of the upper computer, and record and analyze the experimental data in the same way.

Figure 9 depicts the data curve of the yaw - keeping function of the ROV. During the yaw - keeping experiment, the ROV system attains a stable state after an adjustment period of 15 seconds. Once stability is achieved, it can effectively maintain the target yaw angle, with the error remaining within the range of ±2°. This experiment validates that the control performance of the ROV's yaw - keeping function is satisfactory and meets both the design specifications and operational requirements.

5. Conclusions

This paper conducts research on the ROV's motion control technology, establishes a mathematical model, studies the control algorithms, designs controllers, and conducts simulation analysis. The conclusions are as follows:

The sliding mode controller outperforms the classical PID and fuzzy PID controllers in terms of settling time and overshoot.

The control effects of the ROV's depth - keeping and yaw - keeping functions are good, meeting the requirements of actual operations.

The experiment verifies the effectiveness and robustness of the sliding mode control algorithm in the control of underwater robots.

References

[1] Li S, Wu Y, Li C. Application and Prospect of Unmanned Underwater Vehicle [J]. Bulletin of the Chinese Academy of Sciences, 2022, 37(07): 910-920.

[2] Xu Y, Du J, Lei Z. Review: Applications Status and Key Technologies of Underwater Robots in Fishery [J]. Robot, 2023, 45(01): 110-128.

[3] Dalhatu A A, de Azevedo R C, Udebhulu O D, et al. Recent developments of remotely operated vehicles in the oil and gas industry[J]. Holos, 2021, 3: 1-18.

[4] Mazzeo A, Aguzzi J, Calisti M, et al. Marine robotics for deep-sea specimen collection: A systematic review of underwater grippers[J]. Sensors, 2022, 22(2): 648.

[5] Qi S, Yin B, Su Z. Simulation of small-size ROV's specified-depth motion control based on fuzzy PlD [J]. Modern Electronics Technique, 2020, 43(02): 20-23+28.

[6] Dong J, Duan X. Robust Control via a Fuzzy System with PID for the ROV[J]. Sensors, 2023, 23(2): 821.

[7] Wang M. Research on trajectory tracking of underwater vehicle aquaculture cage inspection based on model prediction [D]. Dalian Ocean University, 2022.

[8] Long C, Qin X, Bian Y, et al. Trajectory tracking control of ROVs considering external disturbances and measurement noises using ESKF-based MPC[J]. Ocean Engineering, 2021, 241: 109991.

[9] Prasad M, Swarup A. Position and velocity control of remotely operated underwater vehicles using model predictive control[J]. 2015.

[10] Yang J, Tian S. Research on Depth Control Algorithm of Underwater Vehicle Based on Theory of Sliding Mode [J]. Computer Measurement & Control, 2017, 25(08): 43-45+57.

[11] Garcia-Valdovinos L G, Fonseca-Navarro F, Aizpuru-Zinkunegi J, et al. Neuro-Sliding Control for Underwater ROV's Subject to Unknown Disturbances[J]. Sensors, 2019, 19(13): 2943.

[12] Wang Z, Liu Y, Guan Z, et al. An adaptive sliding mode motion control method of remote operated vehicle[J]. IEEE Access, 2021, 9: 22447-22454.

[13] von Benzon M, Sørensen F, Liniger J, et al. Integral Sliding Mode control for a marine growth removing ROV with water jet disturbance[C]//2021 European Control Conference (ECC). IEEE, 2021: 2265-2270.

[14] Shen Y. Control System of Autonomous Underwater Vehicle Based on Active Disturbance Rejection Control [D]. Northeast Petroleum University, 2015.

[15] Chen Z, Song W, Sun M. Active disturbance rejection control of autonomous underwater vehicles [J]. Journal of Harbin Engineering University, 2021, 42(11): 1625 - 1631.